

Controlled delivery of cytokine growth factors mediated by core–shell particles with poly(acrylamidomethylpropane sulphonate) shells†

Laura Platt, Laura Kelly and Stephen Rimmer*

Cite this: *J. Mater. Chem. B*, 2014, 2, 494Received 30th August 2013
Accepted 22nd November 2013

DOI: 10.1039/c3tb21208d

www.rsc.org/MaterialsB

Core–shell particles have been prepared by surfactant-free emulsion polymerisations of butyl methacrylate in the presence of either linear or highly branched poly(acrylamidomethylpropane sulphonate)s (L-PAMPS or HB-PAMPS) with dithioate end groups: using a “shell-first” approach. In this method the water soluble PAMPS shells were anchored to the cores by polymerisation of BMA from the chain ends. The linear PAMPS produced non-crosslinked poly(AMPS-BMA) particles but the multiple chain ends of the highly branched PAMPS led to crosslinked particles. The particles were loaded with vascular endothelial growth factor or platelet derived growth factor, both of which are cytokines that are known to be important in the production of new blood vessels. The release of the growth factors was shown to be controlled by the architecture of the shell and we propose a mechanism that involves both ionic interaction of the PAMPS with the heparin-binding domains of the growth factors and size exclusion mediated diffusion.

Introduction

Core–shell particles, with distinct phase separated regions (the core and the shell) that have different structures and properties are important components of some key technologies including: paints;¹ adhesives² and toughened plastics³ as well as emergent fields such as controlled delivery of drugs/bioactive compounds.^{4–7} Also, developing a vascular system within tissue engineered or healing tissue is one of the key goals of regenerative medicine and controlling the temporal and spatial availability of key peptide growth factors, such as VEGF, is a vital aspect.⁸ Within this system the action of most of the growth factors involved in angiogenesis involves binding to the highly sulphonated biomacromolecule heparin, *via* highly basic amino acid sequences. With this in mind we reasoned that other sulphonated materials might perform a similar function and that control of the architecture of these polymers could allow for control of delivery. Our aim in this work was to provide a form of a sulphonated polymer with the capacity to control the deliver of growth factors. Therefore, here we report the synthesis of core–shell particles that have shells composed of poly(acrylamidomethylpropane sulphonate) (PAMPS), with two different architectures. The synthesis method makes use of the incorporation of pre-formed polymers with dithioate end groups, in emulsion polymerisations. Two types of architectures

were produced: (1) where the shell was composed of linear-grafted PAMPS (L-PAMPS) attached by one of the chain ends to the core and (2) where the shell was composed of a highly-branched PAMPS (HB-PAMPS) attached to the core by a fraction of the chain ends. These core-branched-shell particles had not been prepared previously and we investigated the hypothesis that control of the availability of growth factors could be achieved by using PAMPS shells of differing architecture. The linear-grafted chains would provide a loose and open set of charged segments whereas the HB-PAMPS shells would be composed of a much denser charged mesh.

We reasoned that higher molar mass peptides would be less able to penetrate into the highly-branched/crosslinked shell so that they would be loaded in the outer regions of the shell only and released with a different profile to smaller peptides. On the other hand shells composed of linear-grafted chains would provide more accessible environments and, therefore, definition of architecture could be used to control the temporal availability of the growth factors.

Typically, many core–shell particles are prepared by emulsion polymerisation of water immiscible monomers and the location of the polymer (core or shell) is dictated by both the sequence of addition and the relative hydrophilic/hydrophobic nature of the monomer and polymer. However, emulsion copolymerisation with water-soluble monomers is very difficult and often it is only possible to incorporate small amounts into otherwise water-immiscible monomer feeds. Also, shells that are water-soluble require some form of attachment to the core or crosslinking to prevent dissolution of the shell. Water soluble shells can be prepared from reactive preformed polymers such as macroinitiators/macro-transfer agents or macromonomers.⁹

The Polymer and Biomaterials Chemistry Labs, Department of Chemistry, University of Sheffield, Sheffield, South Yorkshire, S3 7HF, UK. E-mail: s.rimmer@sheffield.ac.uk; Tel: +44 114 222 5965

† Electronic supplementary information (ESI) available: Data in Fig. 5 represented to show comparisons between thicknesses of shells. See DOI: 10.1039/c3tb21208d

Macroinitiators/macro-transfer agents, with trithiocarbonate or dithioate end groups have been incorporated into emulsion polymerisations^{10–21} and in water these form block copolymers, with hydrophobic monomers, which self-organise into core-shell structures. Also, advances in radical polymerisation have allowed for the synthesis of highly/hyper branched polymers with chain-end functionality that is capable of further polymerisation.²² We considered that the use of these multi-functional macroinitiator/macro-transfer agents in emulsion polymerisation would be useful for the preparation of new core-shell particles in a “shell-first” approach.

The HB-PAMPS was prepared by self-condensing vinyl polymerisation (SCVP),²³ involving the polymerisation of functional monomers, such as **1** in Fig. 1. The use of **1** provides branches that are initiated from chains that are still propagating and this leads to highly/hyper branched architecture. Dithioate-functional monomers have been used to produce a number of highly-branched polymers with useful chain end functionalities using radical addition-fragmentation chain transfer self-condensing vinyl polymerisation (RAFT-SCVP).^{24–28} Here we also consider a method that involves polymerisation of a water immiscible monomer in the presence of a preformed highly-branched water soluble polymer with dithioate chain ends, for preparing core-shell particles with water soluble functional shells. In contrast to the traditional divergent route to core-shell particles, in which the core is prepared then the shell is built around the core, this method involves convergent methodology in which the shell is prepared first followed by the core. We show how shells of poly(2-acrylamido-2-methylpropane sulphonic acid) (PAMPS) can be prepared by first synthesising HB-PAMPS then incorporating this polymer into emulsion polymerisations of butyl methacrylate (BMA). Emulsion polymerisations in the presence of linear macro RAFT agents have only recently been studied but there are no reports of highly-branched macro RAFT agents, such as HB-PAMPS, being used.

One of our key objectives in regenerative medicine is to control angiogenesis and most biomaterials strategies directed at this goal employ heparin to bind growth factors. Binding to heparin increases the stability of growth factors such as the vascular endothelial growth factor (VEGF), platelet derived growth factor (PDGF), *etc.* and controls their availability. Sulphonated polymers such as PAMPS can provide the same function and here we show how these core-shell particles can be used to control the release of VEGF or PDGF.

Results

Fig. 1A shows the route to HB-PAMPS using RAFT-SCVP. Polymerisation of AMPS in the presence of **1** produced the polymer shown in Table 1. The RAFT process using the dithioate ester **2** was also used to produce linear polymer with the reactive chain ends as shown in Fig. 1B. Both the HB-PAMPS and L-PAMPS were prepared with the same fraction of dithioate and monomer in the feed and the same initiator : dithioate ratio. This formulation provided an experimental design in which equal masses of the reaction mixtures for HB-PAMPS and L-PAMPS contain similar amounts of dithioate groups but both the target architectures differed. However, despite the equivalent formulation of the reaction mixtures, ¹H NMR showed that the resultant functionality (*F* in Table 1) of the two polymers was substantially different and this difference arises because the HB-PAMPS synthesis is a copolymerisation whereas the L-PAMPS preparation is a homopolymerisation. The molar mass averages were obtained by aqueous size exclusion chromatography (SEC) using columns packed with a porous polystyrene sulphonate stationary phase. The data are relative to poly(acrylic acid) standards. The intrinsic viscosities [η] in aqueous 1 mol dm⁻³ NaCl are also included in Table 1 and these data were used to confirm the relative size of the two polymers and to calculate the viscosity average molar mass, M_v . In aqueous 1 mol dm⁻³ NaCl, the Mark-Houwink constants (K and α in [η] = KM_v^α) are reported to be $K = 3.6 \times 10^{-5}$ and $\alpha = 0.77$,³² which for L-PAMPS gives $M_v = 12\,100$ g mol⁻¹. Given the non-absolute nature of the SEC measurements this is consistent with the SEC derived value for M_w , shown in Table 1, for this polymer. However, the SEC data for the HB-PAMPS material provide an underestimate of the molar mass averages because of the branched nature of the polymer. The intrinsic viscosity and NMR (degree of branching) data showed the expected trends: that is the L-PAMPS material is a low molar mass oligomeric material and the HB-PAMPS is a higher molar mass material.

The emulsion polymerisation formulations are given in Table 2. These polymerisations (at 60 °C) of BMA in the presence of HB-PAMPS or L-PAMPS produced colloidally stable latexes. However, polymerisations carried out with linear poly(AMPS-*co*-styrene) (in which the styrene contents were equivalent to the aryl contents derived from the RAFT agents in HB-PAMPS and L-PAMPS) prepared by conventional, non-controlled, radical polymerisation produced flocculated masses of polymer in water.

The presence of the dithioate end groups in both HB-PAMPS and L-PAMPS anchored the PAMPS materials to the PBMA cores

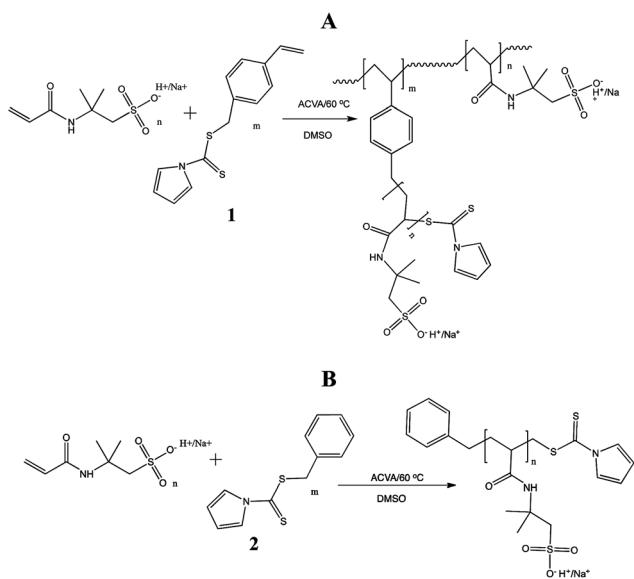


Fig. 1 Synthesis of (A) HB-PAMPS by RAFT-SCVP and (B) L-PAMPS by RAFT.

Table 1 Reaction feeds and characterisation data for L-PAMPS and HB-PAMPS

id	[1] ^a	[2] ^a	[AMPS] ^a	Con ^b	M _n ^c	M _w ^c	[η] ^d	DB ^e	F ^f
L-PAMPS	0	0.062	1.533	99	2400	10 900	0.05 ± 0.002	0	0.87
HB-PAMPS	0.062	0	1.553	96	12 000	23 500	0.11 ± 0.02	0.09	0.06

^a mol dm⁻³. ^b %conversion obtained by gravimetry. ^c g mol⁻¹. ^d Solvent = NaCl_{aq}, 1 mol dm⁻³. ^e DB = degree of branching (branch points per repeat unit). ^f Functionality/mmol of dithioate per unit mass (g).

Table 2 Formulation of the emulsion polymerisations

id	HB-PAMPS/g	L-PAMPS/g	BMA/cm ³	Water/cm ³	K ₂ S ₂ O ₈ /g
HB-A	1	—	100	500	1.2
HB-B	4	—	100	500	1.2
L-A	—	1	100	500	1.2
L-B	—	4	100	500	1.2

as the dithioate end groups transferred and reinitiated during the polymerisation of BMA, producing poly(AMPS-*block*-BMA) sequences. Fig. 2 shows a schematic diagram of the emulsion polymerisation process and includes bimolecular termination reactions that would lead, in the case of HB-PAMPS systems, to the production of crosslinked particles. Crosslinking of the PBMA cores would lead to insoluble materials and this was observed in all polymerisations containing HB-PAMPS. On the

other hand biomolecular termination reactions in the polymerisations containing L-PAMPS, prepared by RAFT, produced triblock copolymers that were not crosslinked and were fully soluble.

Fig. 3 shows scanning electron micrographs of the particles produced with both HB-PAMPS and L-PAMPS. Staining with uranyl formate allowed us to develop electron contrast and the images showed that each reaction produced uniform spherical particles. The images also provided some evidence of the core-shell structure and indicate that the HB-PAMPS particles were smaller (for the same feed of PAMPS) than the L-PAMPS. The main distribution of particles in each sample was around diameters of 150–250 nm but it was possible to discern another distribution that had much smaller diameters. Phase analysis light scattering (PALS) measurements on the same samples allowed us to precisely determine the distributions of particle sizes. The data shown in Fig. 4C, D, G and H confirmed the images and showed that the main distribution of particles had

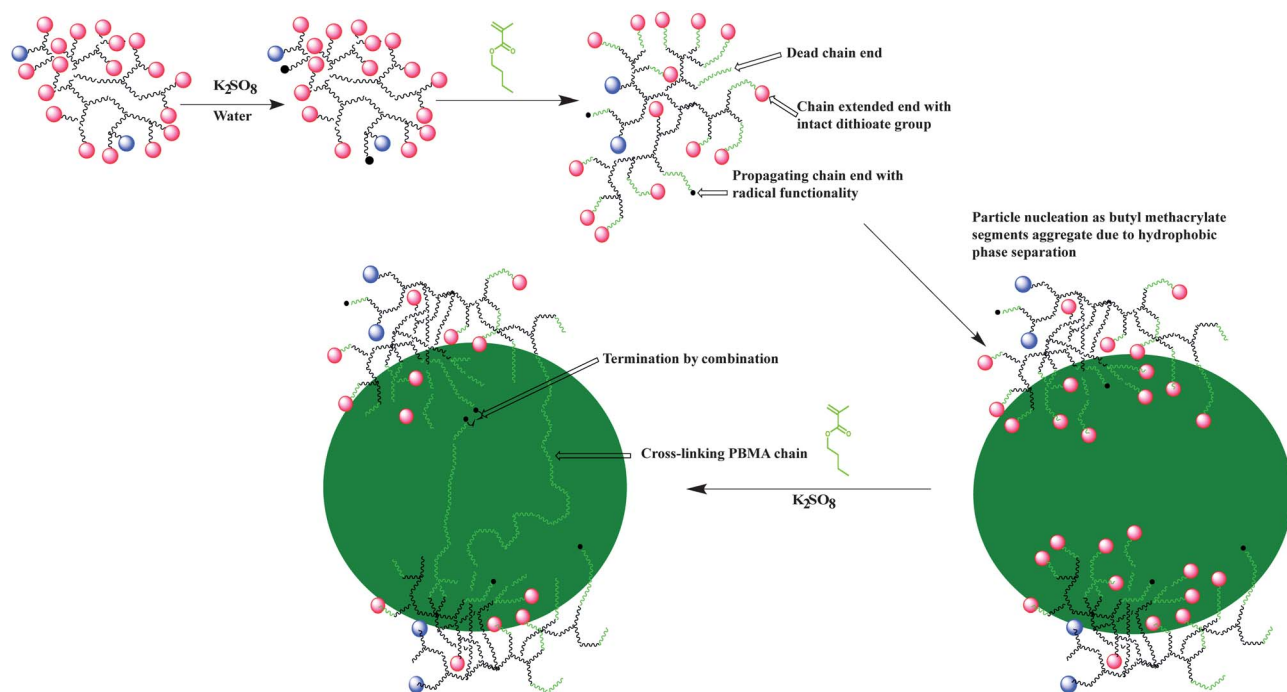


Fig. 2 A schematic diagram showing how polymerisation of a monomer in aqueous emulsion in the presence of a highly branched polymer with dithioate end groups leads to core-shell latex particles. Initially, primary radicals in the aqueous phase react with the dithioate ends (● → ●). These chain-end radicals then react with a hydrophobic monomer. As chain extension ensues eventually the hydrophobic chains aggregate to form particles with the hydrophobic sequences in the core and the HB-PAMPS in the outer shell. Crosslinking of the particles occurs by bimolecular termination.

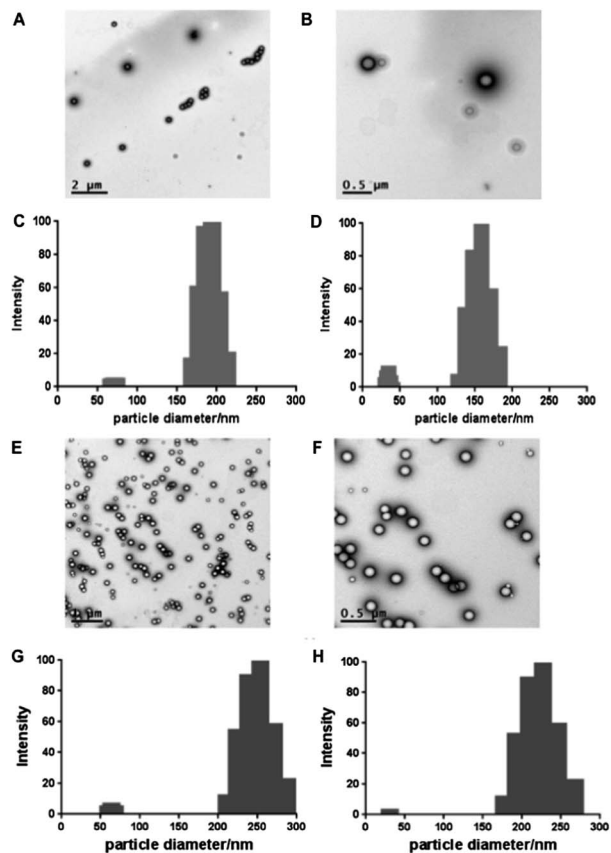


Fig. 3 (A and B) TEM micrographs (stained with uranyl formate) of HB-PAMPS PBMA latex particles. (C) HB-A particle size distribution and (D) HB-B particle size distribution. (E and F) TEM micrographs (stained with uranyl formate) of L-PAMPS PBMA latex particles. (G) L-A particle size distribution and (H) L-B particle size distribution.

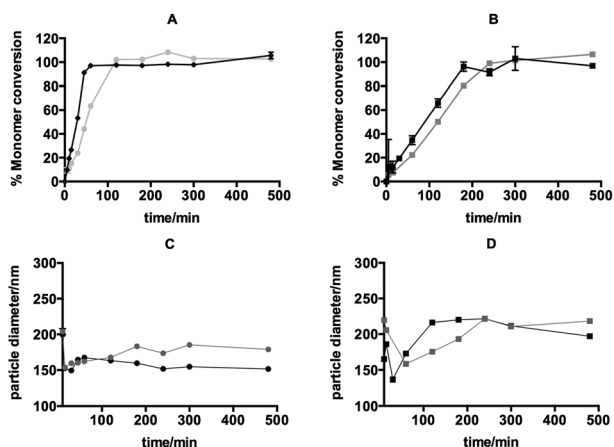


Fig. 4 Plots of conversion/time and particle size/time for emulsion polymerisations of BMA containing HB-PAMPS or L-PAMPS. (A) Conversion of BMA and C, average particle diameter *versus* time for polymerisations containing HB-PAMPS. (B) Conversion of BMA and D, average particle diameter *versus* time for polymerisations containing L-PAMPS: ● HB-PAMPS 1 g; ● HB-PAMPS 4 g; ■ L-PAMPS 1 g; ■ L-PAMPS 4 g.

Table 3 Zeta potentials and final pH of the latexes

	ζ -Potential/mV	Final pH
HB-A	-43.3 ± 3.91	2.8
HB-B	-52.08 ± 2.1	2.3
L-A	-51.91 ± 3.02	2.5
L-B	-30.43 ± 6.26	1.7

peak average diameters between 150 and 250 nm. The main distributions had relatively narrow dispersity (dispersities were 0.20 to 0.26 by PALS) but a second minor distribution was also present in each of the samples, with diameters between 40 and 70 nm. Table 3 also provides the zeta potentials of the final latex particles and these were comparable to electrostatically stabilised sub-micron particles prepared by conventional (prepared with anionic surfactants) means. The latexes also showed the low pHs that are typical of latexes initiated with persulphate.

The emulsion polymerisations incorporating HB-PAMPS and L-PAMPS progressed by different kinetics, as shown in Fig. 4.

Fig. 4A and B show that the polymerisations were much faster when carried out in the presence of HB-PAMPS rather than L-PAMPS. Two weight concentrations of PAMPS were used for each of the HB-PAMPS and L-PAMPS systems but, although the weight concentration of the polymer was kept the same in two instances, the concentration of RAFT agent differed. Thus, the L-PAMPS polymerisations contained higher molar concentrations of dithioate (L-A = 1.5 & L-B = 6.0 mmol dm⁻³) than the HB-PAMPS polymerisation (HB-A = 0.10 & HB-B = 0.4 mmol dm⁻³). These differences can be used to rationalise the lower rates of polymerisations observed with L-PAMPS compared to HB-PAMPS polymerisations: increased concentration of dithioate leading to decreased rates of polymerisation. However, all of the polymerisations progressed to complete conversion within 4 hours. Fig. 4C and D show the evolution of particle size (PALS) over time. By reference also to Fig. 4A and B, we can see that in each reaction the particles reached their maximum average size around 100% conversion and did not increase in size once the reactor was left heated and stirred after all of the monomer had been polymerised. Also, both of the polymerisations containing HB-PAMPS provided smaller particles than the polymerisations containing L-PAMPS. Finally, in the early stages of the polymerisations containing L-PAMPS the average particle size decreased as the reaction progressed but then at higher conversions the particle size increased.

Delivery of heparin binding growth factors

During the development of blood vessels a complex mixture of cytokines control the progress of the emergent vessels. Successful blood vessel formation is affected by the time dependant and spatially resolved concentration of these key proteins. Among the most important of these are VEGF and PDGF. Both VEGF and PDGF are highly unstable *in vivo* with very limited lifetimes.²⁹⁻³¹ Also, it is well-established that the sulphated glucosamino glycan, heparin, plays a role in these cellular processes. However, although binding of these

cytokines to heparin is clearly important the exact role of this binding is unclear. In the absence of heparin the half-lives of VEGFs and PDGFs at 37 °C is typically less than 1 hour. These short half-lives have meant that delivery to wound sites in the hope of initiating development of the vascular system, which is essential for many regenerative medicine strategies, has always failed. Heparin or heparin mimetics appear to be essential in the production of a vascular system and many examples of the use of heparin functionalised materials are available.

However, simply attaching heparin to a surface relies on the hope that the degree of sulphation and binding characteristics of these very heterogeneous materials will be optimum. An important aspect that has never been addressed in these heparin-based materials is that crosslinking can contribute to control the release of growth factors. On the other hand synthetic mimics of heparin, such as PAMPS, as well as having reproducible properties, can provide materials with easily controllable crosslink densities. Our aim in producing these core-shell PAMPS particles was to attempt to control the release of VEGF and PDGF using the architecture of the shell. In the longer term it is our intention to use the particulate core-shell design to enable the use of these materials as functional additives in other commodity bio-medical materials.

In each release study 100 ng of VEGF-165 or PDGF-BB was added to 0.5 ml of latex (= 100–200 mg of polymer). ELISAs of the supernatants after coagulation of these latexes showed that 97–99% of the growth factors was absorbed by the particles. Fig. 5 shows the results from experiments designed to monitor the release (using ELISA to quantify the amount of growth factor released over a period of 33 days) of both VEGF 165 and PDGF-BB: the two most commonly studied variants of these key growth factors. Fig. 5A and B show the data for the release of VEGF-165. The first observation to be made on these data is that there are significant differences (repeated measures analysis of variance with Tukey *post-hoc* analysis) in the release profiles, between the linear-grafted shells compared to the highly-branched/crosslinked shells. On the other hand comparisons of

the release based on the amount PAMPS (*i.e.* comparisons between the two L-PAMPS shells and comparisons between the two HB-PAMPS shells (see ESI†)) in the shell provided no significant differences in behaviour. The data showed that the architecture of the shell not only influences the amount of VEGF released but also that the release from the HB-PAMPS shells was essentially finished by 200 hours: although a very slow release continued from the larger shell materials. On the other hand shells prepared with the L-PAMPS released material in an almost linear and continuous manner over the full 800 hours of the experiment. The shells did show a small burst release for the initial 24 hour period but then this was followed by a long period of continuous release. Notably the release from the linear-grafted shells was slower over the first 200 hours than from the highly-branched/crosslinked shells. However, after this time the release from the highly-branched/crosslinked shells became exhausted and the rate of release was slower than from the linear-grafted shells. Fig. 5C and D show the release of the PDGF-BB from the same particles. As with the VEGF experiments there were no significant effects of changing the amount of PAMPS in the feed (see ESI†).

However, the effects of shell architecture were highly significant. The data also showed that, with each core-shell material, the release of PDGF-BB was slower than the release of VEGF 165. However, unlike in the data from the release of VEGF 165 the release of PDGF-BB from the linear-grafted shells remained less than from the highly branched/crosslinked shells though out the time course of the experiment.

Discussion

We have shown how we can prepare sub-micron particles, which could be used as additives during the processing of other materials, that control the availability of growth factors. Although, aqueous polymer emulsions have been prepared using linear poly(acrylic acid)s with dithiocarbonate end groups to produce block copolymer stabilisers, this is the first time that a charged or hydrophilic branched polymer has been polymerised in emulsion polymerisation with a hydrophobic comonomer. This “shell-first” approach to core-shell particles is a useful method of attaching an otherwise water-soluble shell to a polymer particle. Emulsion polymerisations with a linear PAMPS version of the previously published linear PAA stabilisers had not been reported and these were also shown to be effective at mediating the emulsion polymerisation of BMA. Although, not included here we also attempted to use a highly-branched PAA in this system, at a variety of reaction pHs but all our attempts to prepare stable colloids failed. The particles produced with HB-PAMPS were colloiddally stable and crosslinked.

Similar, homogenous polymer microgel-particles have been well studied as drug delivery vehicles but PAMPS microgels have hardly been reported. The results reported here have shown how different growth factors can be delivered at different rates and since both the spatial and temporal availability of these cytokines is important *in vivo* we believe that this is a key advance in the area. Heparin based biomaterials have been well-

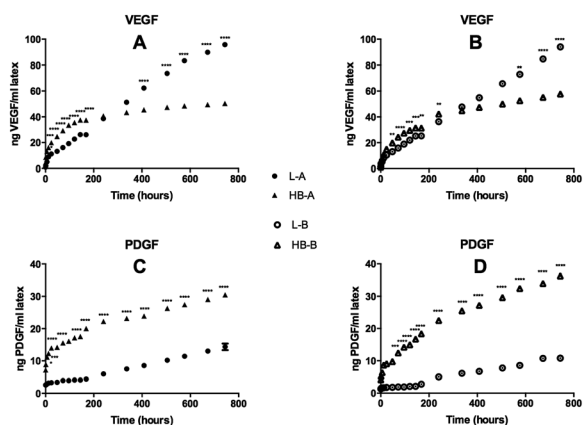


Fig. 5 Release of VEGF 165 and PDGF-BB from L-PAMPS and HB-PAMPS particles: VEGF 165 released from particles formed from, (A) 1 g and, (B) 4 g of PAMPS added to the feed; PDGF-BB released from particles formed from, (C) 1 g and, (D) 4 g of PAMPS.

studied for modifying the stability and availability of heparin binding growth factors of importance in angiogenesis. However, although it is clear that heparin plays a role these materials have not been shown to control the delivery of growth factors. Also, it is difficult to deploy heparin without covalent or electrostatic attachment to a device, which can add significant complications to manufacturing processes. It is probable that if facile routes to controlling the architecture of heparin could be designed then the size exclusion/electrostatic control could also be provided with these polyelectrolytes. At the current time the required heparin-based structures are not available. However, Tsurkin *et al.* recently reported a procedure for producing poly(ethylene glycol)/heparin conetwork particles by grinding bulk materials: a process that, in comparison to emulsion polymerisation, is difficult to scale-up.³⁴ These authors reported that release of basic fibroblast growth factor or epidermal growth factor occurred over approximately 40 hours, which is a similar timescale to the release kinetics that we reported for VEGF from a poly(*N*-vinyl pyrrolidone-heparin) network with heparin bound electrostatically.³⁵ Controlling, the availability of growth factors is clearly important in angiogenesis and, typically, VEGF is required early in blood vessel development but then at later time points other growth factors such as PDGF play key roles as the vessels mature.³³ Here we have shown that we can provide different release profiles of these two growth factors and that it is possible to design materials that can deliver VEGF at early time points as well as materials that produce a much slower release of PDGF over a longer time period. The recombinant VEGF-165 used in this work is a homodimeric protein with a molar mass of 38.2 kg mol⁻¹ and the PDGF-BB is also a homodimeric protein but with a lower molar mass: 24.3 kg mol⁻¹. Both of these cytokine growth factors have affinity, which is mediated by highly basic amino sequences, for heparin. Thus, apart from the detail of the amino acid sequences, the key difference between these two proteins is their size and it seems reasonable to propose that the differences in release behaviour are related to size exclusion effects. At the concentrations of relevance to this and the *in vivo* situation there was an excess of sulphonate groups, which can provide a sufficient density of binding sites to effectively sequester both growth factors in the outer regions of all of the shells. However, penetration into the shell would be dependent on the size of the growth factor and the architecture of the shell: larger molar mass and increased crosslink density both can act to decrease diffusion into the shell. Similarly, diffusion out of the shell by growth factors that have penetrated deeply would be more hindered by a branched/crosslinked shell rather than a linear-grafted shell. Thus, in the case of VEGF 165 both the linear grafted and the branched/crosslinked systems would be expected to absorb the growth factor but then its release would be at a significantly faster rate from the branched/crosslinked shell because it would be released from the outer regions of the shell rather than from more evenly across the depth of the shell. In this proposed model, VEGF 165 would have been absorbed onto the branched/crosslinked shell but its relatively large size would prevent its penetration into the shell. However, although the release was faster, at early time points, from highly

branched/crosslinked shell it slowed after 200 hours. Given the requirements for VEGFs early in the angiogenesis process the highly branched/crosslinked shells appears to provide a more appropriate release behaviour than the linear-grafted shells, for VEGF 165. However, PDGF-BB is required over a much longer time scale *in vivo* and the data showed that the highly branched/crosslinked shells released PDGF-BB with an initial burst release whereas the linear-grafted shells provided a steady release through out the 800 hours of the experiment. Thus, it appears that by tuning the architecture of a sulphonated shell it is possible to design particles that release growth factors at rates that are close to the *in vivo* requirements for angiogenesis. Clearly, further formulation with *in vitro* and *in vivo* testing will be required to provide optimised angiogenic delivery systems but the particles described here have been shown to provide excellent control of the delivery of two of the most important growth factors involved.

Conclusion

Core-shell particles with polysulphonate shells were prepared by a shell-first approach. Shells composed of poly(acrylamidomethylpropane sulphonate) with either linear grafted or highly-branched/crosslinked architectures were prepared and it was shown that the release of two heparin binding growth factors was dependant on the architecture of the charged shells.

Experimental

Instrumentation and analysis

NMR. Proton and carbon NMR experiments were run using a Bruker Avance 400 Spectrometer, 400 MHz. Deuterated chloroform and dimethyl sulphoxide were used as sample solvents.

Solid content. Latexes were analysed to determine solid content by measuring the mass of latex and then drying to constant mass in a vacuum oven (40 °C).

Solid content (%) = (mass of dry latex/mass of wet latex) × 100

Particle size. Brookhaven Instruments zeta potential analyser using ZetaPALS particle size analyser software was used to measure mean particle sizes, particle size distributions and zeta potentials of the latexes. For particle size analysis the samples were diluted using 10 mmol potassium chloride prior to analysis. For zeta potential measurements the samples were diluted using 1 mmol potassium chloride prior to analysis and the instrument was standardised using BI-ZR3 reference material before each set of samples. Reference conductance was measured as 320 μS ± 30.

THF SEC. Analysis of soluble PBMA samples (from emulsion polymerisations made with L-PAMPS) was undertaken using filtered (0.45 μm vacuum filtration) GPC grade THF (stabilised with 250 ppm BHT) (Fisher) as the mobile phase, three high molecular weight columns (PL mixed 'B') and a refractive index detector were used. The instrument was calibrated using poly(styrene) standards. GPC grade toluene was

used as a flow rate marker and samples were filtered through a 0.45 μm PTFE syringe filter before injection. Eluent flow rate was 1 ml min^{-1} .

Aqueous SEC. Analysis of L-PAMPS and HB-PAMPS was undertaken using filtered (0.45 μm vacuum filtration) 0.08 M TRIS/0.15 M NaCl prepared with millipore water (18.2 $\text{M}\Omega\text{ cm@}25^\circ\text{C}$) as the mobile phase, Jordi Gel DVB Sulphonate GPC columns with a refractive index detector. The instrument was calibrated using poly(acrylic acid) standards (Agilent). Samples were prepared at 1 mg ml^{-1} concentration and filtered through a 0.45 μm PTFE syringe filter before injection. Eluent flow rate was 1 ml min^{-1} .

Microscopy. Transmission electron microscopy (TEM) was carried out using a FEI Tecnai Spirit Microscope operating at 100 kV. Latex samples (50 μl) were loaded onto gold mesh sample mounts, left for approximately one minute and the excess water removed by blotting. These were then allowed to air dry. Samples were stained with uranyl formate solution in water and allowed to dry fully before examination by TEM.

Dilute solution viscometry. The viscosities of polymer solutions of varying concentrations (g dL^{-1}) were measured using an Ubbelohde viscometer (Rheotek PSL 1 68035). Solutions were made using 1 M sodium chloride (VWR, 99.7%) made using millipore water (18.2 $\text{M}\Omega\text{ cm@}25^\circ\text{C}$). A known volume of polymer solution was charged to the viscometer and internal dilutions carried out (10 ml of starting stock solution with solvent dilutions). A viscometric water bath (Rheotek) at $25^\circ\text{C} \pm 0.2^\circ\text{C}$ was used for all measurements with samples equilibrated for 15 minutes prior to measurements. All measurements were repeated in triplicate to ± 0.05 s.

Highly branched poly(2-acrylamido-2-methyl-1-propane-sulphonic acid) using 4-vinylbenzyl-1-pyrrolocarbodithioate as a chain transfer agent. 2-Acrylamido-2-methyl-1-propane-sulphonic acid (Sigma Aldrich, 99%), 4,4'-azobis(4-cyanovaleric acid) (Sigma Aldrich, $\geq 98\%$) and 4-vinylbenzyl-pyrrolocarbodithioate were dissolved in anhydrous DMSO (20 ml) using a molar ratio of 25 : 1 AMPS monomer to chain transfer agent. The yellow solution was transferred to a glass ampoule (50 ml). The ampoule was evacuated using a hi-vacuum line (10^{-3} mbar), a freeze-pump-thaw cycle was repeated $\times 3$. The ampoules were sealed with a flame and placed in a water bath at 60°C for 24 hours. The polymer solution was precipitated into acetone (800 ml). The acetone was decanted off and evaporated and the polymer washed with distilled water. The wet polymer was freeze dried to give a yellow solid.

$^1\text{H NMR}$ (400 MHz, $(\text{CD}_3)_2\text{S=O}$) (ppm): δ 8.02 (br), δ 7.46 (br, Ar), δ 5.98 (1H, br, RCH=CH), δ 5.56 (1H, br, RCH=CH), δ 3.34 (2H, br, $\text{CH}_2\text{CH}_2\text{SCO}$), δ 2.72 (2H, br, $\text{RCH}_2\text{SO}_3\text{H}$), δ 2.53 (2H, br, RCH_2CH_2), δ 2.09 (1H, br, RCOCH), δ 1.32 (6H, br $\text{CH}(\text{CH}_3)_2$).

$^{13}\text{C NMR}$ (400 MHz, $(\text{CD}_3)_2\text{S=O}$) (ppm): δ 206.50 (RC=S), δ 173.44 (RC=O), δ 164.79 ($\text{RSCH}_2\text{C=O}$), δ 133.65 (Ar), δ 124.45 (Ar), δ 58.86 ($\text{RCH}_2\text{SO}_3\text{H}$), δ 52 (RCHS), δ 33.07 (RCH_2), δ 31.15 (RCH_2), δ 27.31 (RCH_3).

Linear poly(2-acrylamido-2-methyl-1-propane sulphonic acid) using benzyl-1-pyrrolocarbodithioate as a chain transfer agent. L-PAMPS was prepared as HB-PNIPAM but benzyl-1-pyrrolocarbodithioate was used as the transfer agent.

$^1\text{H NMR}$ (400 MHz, $(\text{CD}_3)_2\text{S=O}$) (ppm): δ 10.12 (1H, br, RNH), δ 7.27 (6H, br, Ar), δ 6.41 (2H, br, Ar), δ 5.98 (1H, br, RCH=CH), δ 5.50 (1H, br, RCH=CH), δ 3.31 (2H, br, $\text{CH}_2\text{CH}_2\text{SCO}$), δ 2.40 (2H, br, RCH_2CH_2), δ 1.99 (1H, br, RCOCH), δ 1.23 (6H, br $\text{CH}(\text{CH}_3)_2$).

$^{13}\text{C NMR}$ (400 MHz, $(\text{CD}_3)_2\text{S=O}$) (ppm): δ 173.44 (RC=O), δ 128.02 (Ar), δ 59.96 ($\text{RCH}_2\text{SO}_3\text{H}$), δ 52.55 (RCHS), δ 39.92 (RCH_2), δ 31.70 (RCH_2), δ 25.11 (RCH_3).

Emulsion polymerisation of *n*-butyl methacrylate using HB-PAMPS and L-PAMPS. BMA (Sigma Aldrich, 99%) was vacuum distilled before use. Ultrapure water (18.2 $\text{M}\Omega\text{ cm@}25^\circ\text{C}$), BMA and varying amounts of HB-PAMPS or L-PAMPS were charged to a 1 L jacketed reactor fitted with a nitrogen inlet, overhead stirrer, condenser and heated water circulator. BMA was added last with vigorous stirring to form a quasi-stable emulsion. The reactants were stirred and purged with nitrogen for approximately one hour before commencing the reaction. The reaction vessel was heated to 60°C and potassium persulphate (Sigma Aldrich, $\geq 99\%$) solution (purged with nitrogen) was introduced. Samples (approximately 20 ml) in order to assess monomer conversion rate were taken from the reaction vessel at various time intervals and quenched using hydroquinone monomethyl ether (Sigma Aldrich, $\geq 98\%$). All reactions were carried out for eight hours in total.

The samples using HB-PAMPS were crosslinked and therefore insoluble in all solvents. PBMA latexes using the L-PAMPS were soluble and analysed using NMR and THF SEC, as follows:

$^1\text{H NMR}$ (400 MHz, CDCl_3) (ppm): δ 4.81 (2H, br, RC=OCH₂), δ 4.03 (2H, br, RC=OCH₂), δ 1.88 (2H, br, RCH_2CH_2), δ 1.61 (2H, br, $\text{RCH}_2\text{CH}_2\text{CH}_3$), δ 1.40 (2H, br, $\text{RCH}_2\text{CH}_2\text{CH}_3$), δ 0.88 (3H, br, $\text{RCH}_2\text{CH}_2\text{CH}_3$).

$^{13}\text{C NMR}$ (400 MHz, CDCl_3) (ppm): δ 177.51 (RC=OCH₂), δ 64.71 (RCH_2O), δ 45.44 (RCHC=O), δ 30.29 (RCH_2CH_2), δ 19.32 (RCH_2CH_3), δ 13.75 (RCH_3).

THF SEC (g mol^{-1}).

L-A: M_n 115 800, M_w 300 200, M_z 628 300, polydispersity 2.59.

L-B: M_n 140 600, M_w 241 300, M_z 362 400, polydispersity 1.72.

Release of growth factors

Dialysis of latex. 12–15 kDa dialysis tubing (Sigma Aldrich) was soaked in distilled water for 2 minutes. Excess water was decanted off and each section of tubing was filled, using a syringe, with 20 ml of latex. The latex underwent dialysis in 500 ml distilled water with this solution and was changed twice daily for 6 days.

Protein binding and release studies. 0.5 ml 7 : 3 iPA : H₂O was added to 0.5 ml latex. The samples were agitated for 30 minutes then centrifuged at 13 000 rpm for 30 minutes. The supernatant was removed leaving a solid polymer pellet. 0.5 ml phosphate buffered saline (PBS) was added to the latex solid and agitated for 30 minutes. The sample was centrifuged at 13 000 rpm for 30 minutes and then the supernatant was removed. This process was continued until the supernatant was pH 7. A solution of 100 ng ml^{-1} VEGF-165 (Peprotech) was made up with the inclusion of 1% bovine serum albumin (Sigma Aldrich). 0.5 ml of this solution was added to each of the polymer samples, which were left at 4°C for 18 hours with gentle agitation. The VEGF-165 solution was removed and replaced

with 0.5 ml PBS. The samples were stored at 37 °C for the remainder of the experiment. Samples of supernatant were taken at time intervals and stored at –80 °C until analysis. The same procedure was followed for the binding and release of PDGF-BB.

Enzyme linked immunosorbent assay (ELISA). ELISA was carried out using a VEGF or PDGF sandwich ELISA kit (R&D Systems). The developed plate was read using MRX II plate reader (Dynex Technologies) with correction wavelengths at 540 nm and 450 nm. All samples and standards were analysed in triplicate.

Notes and references

- 1 A. K. Khan, B. C. Ray and S. K. Dolui, *Prog. Org. Coat.*, 2008, **62**, 65.
- 2 R. Mascorro, M. Elena-Navarro, H. Dorantes and M. Corea, *Macromol. Symp.*, 2010, **297**, 69.
- 3 Q. B. Si, C. Zhou, H. D. Yang and H. X. Zhang, *Eur. Polym. J.*, 2007, **43**, 3060.
- 4 Y. Wang, S. Gao, W.-H. Ye, H. S. Yoon and Y.-Y. Yang, *Nat. Mater.*, 2006, **5**, 791.
- 5 R. Haag, *Angew. Chem.*, 2004, **43**, 278.
- 6 D. J. Siegwart, K. A. Whitehead, L. Nuhn, G. Sahay, H. Cheng, S. Jiang, M. Ma, A. Lytton-Jean, A. Vegas, P. Fenton, C. G. Levins, K. T. Love, H. Lee, C. Cortez, S. P. Collins, Y. F. Li, J. Jang, W. Querbes, C. Zurenko, T. Novobrantseva, R. Langer and D. G. Anderson, *Proc. Natl. Acad. Sci. U. S. A.*, 2011, **108**, 12996.
- 7 L. Gilmore, S. MacNeil and S. Rimmer, *ChemBioChem*, 2009, **10**, 2165.
- 8 N. Ferrara, H.-P. Gerber and J. LeCouter, *Nat. Med.*, 2003, **9**, 669.
- 9 S. Rimmer, M. Ramli and S. Lefèvre, *Polymer*, 1996, **37**, 4135.
- 10 C. J. Ferguson, R. J. Hughes, D. Nguyen, B. T. T. Pham, R. G. Gilbert, A. K. Serelis, C. H. Such and B. S. Hawkett, *Macromolecules*, 2005, **38**, 2191.
- 11 C. J. Ferguson, R. J. Hughes, B. T. T. Pham, B. S. Hawkett, R. G. Gilbert, A. K. Serelis and C. H. Such, *Macromolecules*, 2002, **35**, 9243.
- 12 S. Freal-Saison, M. Save, C. Bui, B. Charleux and S. Magnet, *Macromolecules*, 2006, **39**, 8632.
- 13 J. Rieger, G. Osterwinter, C. Bui, F. Stoffelbach and B. Charleux, *Macromolecules*, 2009, **42**, 5518.
- 14 J. Rieger, W. Zhang, F. Stoffelbach and B. Charleux, *Macromolecules*, 2011, **44**, 7584.
- 15 J. Rieger, F. Stoffelbach, C. Bui, D. Alaimo, C. Jerome and B. Charleux, *Macromolecules*, 2008, **41**, 4065.
- 16 M. Manguian, M. Save and B. Charleux, *Macromol. Rapid Commun.*, 2006, **27**, 399.
- 17 I. Chaduc, M. Girod, R. Antoine, B. Charleux, F. D'Agosto and M. Lansalot, *Macromolecules*, 2012, **45**, 588.
- 18 Y. Wi, K. Lee, B.-H. Lee and S. Choe, *Polymer*, 2008, **49**, 5626.
- 19 J. Xu, X. Wang, Y. Zhang, W. Zhang and P. Sun, *J. Polym. Sci., Part A: Polym. Chem.*, 2012, **50**, 2484.
- 20 N. Yeole and D. Hundiwale, *Colloids Surf., A*, 2011, **392**, 329.
- 21 N. Yeole, D. Hundiwale and T. Jana, *J. Colloid Interface Sci.*, 2011, **354**, 506.
- 22 R. M. England and S. Rimmer, *Polym. Chem.*, 2010, **1**, 1533.
- 23 J. M. J. Frechet, M. Henmi, I. Gitsov, S. Aoshima, M. R. Leduc and R. B. Grubbs, *Science*, 1995, **269**, 1080.
- 24 S. Carter, S. Rimmer, R. Rutkaite, L. Swanson, J. P. A. Fairclough, A. Sturdy and M. Webb, *Biomacromolecules*, 2006, **7**, 1124.
- 25 S. Hopkins, S. R. Carter, J. W. Haycock, N. J. Fullwood, S. MacNeil and S. Rimmer, *Soft Matter*, 2009, **5**, 4928.
- 26 J. Shepherd, P. Sarker, K. Swindells, I. Douglas, S. MacNeil, L. Swanson and S. Rimmer, *J. Am. Chem. Soc.*, 2010, **132**, 1736.
- 27 P. Sarker, J. Shepherd, K. Swindells, I. Douglas, S. MacNeil, L. Swanson and S. Rimmer, *Biomacromolecules*, 2011, **12**, 1.
- 28 S. Carter, B. Hunt and S. Rimmer, *Macromolecules*, 2005, **38**, 4595.
- 29 S. M. Jay and W. M. Saltzman, *J. Controlled Release*, 2009, **134**, 26.
- 30 R. Yang and S. Bunting, *J. Pharmacol. Exp. Ther.*, 1998, **284**, 103.
- 31 S. M. Eppler, D. L. Combs, T. D. Henry, L. J. Lopez, S. G. Ellis, J.-H. Yi, B. H. Annex, E. R. McCluskey and T. F. Zioncheck, *Clin. Pharmacol. Ther.*, 2002, **72**, 20.
- 32 L. W. Fischer, A. R. Sochor and J. S. Tan, *Macromolecules*, 1977, **10**, 949.
- 33 W. Risau, *Nature*, 1997, **386**, 671.
- 34 M. V. Tsurkan, P. V. Hauser, A. Zieris, R. Carvalhosa, B. Bussolati, U. Freudenberg, G. Camussi and C. Werner, *J. Controlled Release*, 2013, **167**, 248.
- 35 L. Gilmore, S. Rimmer, S. L. McArthur, S. Mittar, D. Sun and S. MacNeil, *Biotechnol. Bioeng.*, 2013, **110**, 296.